Published in final edited form as:
Bone. 2011 June 1; 48(6): 1362–1369. doi:10.1016/j.bone.2011.03.773.

The expression of osteoprotegerin is required for maintaining the intervertebral disc endplate of aged mice

Qian-Qian Liang, PhD[*,†,‡], **Xiao-Feng Li, MD**[*,†,‡], **Quan Zhou, PhD**[*,†], **Lianping Xing, PhD**[¶], **Shao-Dan Cheng, PhD**[*,†], **Dao-Fang Ding, PhD**[*,†], **Le-Qin Xu, PhD**[*,†], **De-Zhi Tang, PhD**[*,†], **Qin Bian, PhD**[*,†], **Zhi-Jie Xi, PhD**[*,†], **Chongjian Zhou, PhD**[*,†], **Qi Shi, MD**[*,†], and **Yong-Jun Wang, PhD**[*,†]

[*] Department of Orthopaedics & Traumatology, Longhua Hospital, ShangHai University of Traditional Chinese Medicine. Shanghai, 200032, P.R. China

[†] Institute of Spine, Shanghai University of Traditional Chinese Medicine. Shanghai, 200032, P.R. China

[¶] Department of Pathology and Laboratory Medicine, University of Rochester Medical Center, Rochester, NY, 14642, USA

Abstract

Objective—Human chondrocytes and annulus fibrosus cells of intervertebral disc (IVD) express osteoprotegerin (OPG), but the effect of OPG on the pathogenesis of IVD degeneration remains unknown. Here we assessed the phenotype change of IVD in $OPG^{-/-}$ mice.

Methods—The IVDs from 12-, 20-, and 28-week-old $OPG^{-/-}$ mice and WT controls were subjected to histologic analyses including TRAP staining for osteoclasts, immunostaining for OPG and type I collagen protein expression, and TUNEL staining for apoptosis. The IVD tissues were also subjected to real time RT-PCR for mRNA expression of genes for osteoblast-*osterix, ALP,* and *osteocalcin*; for osteoclasts-*trap, rank, mmp9 and cathepsin K*, and for chondrocytes-*aggrecan, mmp13* and *Col10*.

Results—OPG protein expresses at the cells of endplate cartilage and annulus fiborsis in IVDs of WT mice. Compared to WT mice, $OPG^{-/-}$ mice developed aging related cartilage loss and bony tissue appearance at the endplate. Stating from 20 weeks of age, IVDs from $OPG^{-/-}$ mice expressed significantly increased *mmp13* and *Col10* levels, which is associated with increased

Please address correspondence to: Yong-Jun Wang MD, PhD, Institute of Spine, Shanghai University of Traditional Chinese Medicine, 725 Wan-Ping South Road, Shanghai 200032, China, Tel: 0086-21-5423-2267, Fax: 0086-21-6443-4704, yjwang88@hotmail.com.
[‡]Both authors contributed equally to this paper

Competing interests
All authors have no competing interests.

Authors' contributions
QQL drafted the manuscript and analyzed and interpreted the data. XFL acquired the data from histologic analyses, and contributed to drafting of the manuscript. QZ carried out RT-PCR experiment. LPX analyzed and interpreted the data, and contributed to drafting of the manuscript. SDC and DZT conducted genotyping and mouse culture. DFD contributed to drafting of the manuscript. LQX participated in the TUNEL staining experiment. QB, ZJX, CJZ, and QS participated in the conception and design of the study. YJW participated in the conception and design of the study, contributed to analysis and interpretation of data and assisted in drafting the manuscript. All authors approved the final manuscript.

osteoblast number and elevated expression of osteoblast marker genes. Furthermore, TRAP+ osteoclasts were presented in the endplate cartilage of *OPG*$^{-/-}$ mice. These osteoclasts localized adjacently to and erosion into the cartilage. Increased expression of *RANK, mmp9 and cathepsin k* was detected in *OPG*$^{-/-}$ IVDs.

Conclusions—OPG at IVD plays an important role for maintaining the integrity of endplate cartilage during aging by preventing endplate cartilage from osteoclast-mediated resorption.

Keywords

Osteoprotegerin; intervertebral disc; cartilage endplate; osteoclast; intervertebral disc degeneration

Introduction

Osteoporosis and spinal degeneration diseases or intervertebral disc (IVD) degeneration are prevalent skeletal diseases that cause pain, physical limitations, and disability in aged population [1, 2]. Several studies reported the coexistence of osteoporosis and degenerative disc disease, but the relationship between these two diseases remains unclear [3, 4].

Osteoprotegerin (OPG), a naturally occurring inhibitor of the receptor activator of NF-κB ligand (RANKL), binds RANKL with high affinity, preventing RANKL from interaction with RANK on osteoclasts [5]. OPG negatively regulates osteoclast formation and thus prevents the osteoporosis. The imbalance of the RANKL-OPG, caused by estrogen shortage, glucocorticoid application, or immune-mediated disorganizations, would induce osteoclastogenesis and accelerated bone resorption [6]. OPG gene knockout mice (*OPG*$^{-/-}$) develop severe osteoporosis with remarkably increased osteoclast numbers. Furthermore, *OPG*$^{-/-}$ mice also have severe osteoarthritis phenotypes due to completed loss of articular cartilage in knee joints, suggesting OPG may affect the integrity of cartilage. OPG is expressed and produced by many cell types. It was reported that human chondrocytes and annulus fibrosus of IVD express OPG and RANKL [7–9]. However, the effect of OPG on IVDs has not been investigated. Here we directly compared the IVD phenotypes of different ages of *OPG*$^{-/-}$ mice and WT control mice. *OPG*$^{-/-}$ mice develop degenerative disc disease with aging. Thus, the purpose of this study is to investigate the phenotype change of intervertebral discs in OPG gene knock out mice.

Materials and Methods

Animals

OPG heterozygous mice in S129 background were purchased from Shanghai Research Center for Biomodel Organism, China and were bred to generate *OPG*$^{-/-}$ mice. Genotype of *OPG*$^{-/-}$ mice was determined by PCR. The OPG WT allele was detected using the forward primer 5′-GTA ACG CCC TTC CTC ACA CTC ACA -3′ and the revered primer 5′-ATG GCC ATT CAG CAG TAG CCT ATG -3′. The OPG mutant allele was detected by using the forward primer 5′-GTA ACG CCC TTC CTC ACA CTC ACA -3′ and the revered primer 5′-GTG GGG GTG GGG TGG GAT TAG ATA -3′. *OPG*$^{-/-}$ mice and WT littermates (N=6/group) were sacrificed at 12, 20, and 28 weeks of age. The local ethics committee approved all animal procedures.

Histological evaluation

The specimens of the IVD and adjacent endplate cartilage from Cervical (C) vertebral body 4 to C6 were fixed in 4% Paraformaldehyde, decalcified, dehydrated, cleared with dimethylbenzene, and were then embedded in olefin. At least 4 consecutive 7-μm sections were obtained from the coronal planes, and stained using Haematoxylin and Eosin (HE) for

routine morphologic analysis and TRAP staining for identifying osteoclasts. The morphology of the cartilage endplate, annulus fibrous, and nucleus pulposus was examined. Histomorphometric assessment was performed by using an image auto-analysis system (Olympus BX50; Japan).

Immunofluorescence staining of OPG

The paraffin sections of the IVD and adjacent vertebral endplates from C4–C6 of 12-week-old WT mice were deparaffinized, blocked with 0.2% triton 100 for 10 minutes at room temperature, and followed by a digestion with proteinase K in PBS, for about 10 minutes at 37°C. The sections were incubated with 5% BSA for 2 hours at 37°C to block non-specific staining and followed with 1:100 goat polyclonal anti-OPG antibody (sc-8468, Santa cruz biotechnology, CA, USA) at 4°C overnight. After thorough wash with PBS, the sections were incubated with 1:400 rabbit anti-goat IgG secondary antibody labeled with DyLight 680 (072-06-13-06, Kirkegaard & Perry Laboratories, Inc. Maryland, USA) for 45 min, followed with thorough wash with PBS, and mounted. The specimens were observed using an Image Analysis System (Olympus BX50, Japan).

Immunohistochemical staining of type I collagen

The slides were processed the standard program of dewaxing, rehydrating, block endogenous peroxidase 10 minutes in 3% H_2O_2, followed by a digestion with 0.01% protease K for 10 minutes. Non-specific signals were blocked by incubation with confining liquid for 10 minutes. The sections were then incubated with Rabbit polyclonal antibody to type I collagen (abcam, MA, USA), at 4°C over night. After thorough wash, the sections were incubated with biotinylated goat anti-rabbit IgG 10 minutes at 4°C for 60 minutes, and then incubated in Streptavidin-HRP for 10 minutes. The color reaction was elicited by 3,3′-diaminobenzidine (DAB) solution at last. Tematoxylin was used to counterstain the sections. After being mounted, specimens were examined by using an Image Analysis System (Olympus BX50, Japan).

TUNEL staining

Four midsagittal sections of each IVD were stained for dead cells using the TdT-dUTP terminal nick-end labeling (TUNEL) reaction (MEBSTAIN Apoptosis Kit Direct, MA, USA) according to the manufacturer's protocol.

Real-time RT-PCR analysis

Total RNA was extracted from C4–C6 IVD samples by TRIzol reagent (invitrogen Life Technologies, Carlsbad, CA). Reverse transcription was preformed using a RT-for-PCR kit (Qiagen, Valencia, CA) following the manufacturer's protocol. Real-time RT-PCR amplifications were performed using a SYBR Premix Ex Taq (Takara Bio) in the machine RG3000 (Corbett Research, Australia). The primers for real-time RT-PCR used were showed (Table 1). The mRNA expression was normalized to β-actin. PCR products were subjected to melting curve analysis, while the data were quantified using RotorGene 6.0 analysis software. The experiments were repeated at least three times.

Statistical Analysis

One-Way ANOVA, followed with Post Hoc Turkey HSD for multiple comparisons, was performed by using SPSS software (SPSS 10.0, Chicago, IL). Significance was defined by p values <0.05.

Results

Abnormal endplate cartilage and IVD structures in vertebra of adult *OPG*$^{-/-}$ mice

To investigate the involvement of OPG in the development of disc diseases, we examined the expression pattern of OPG in inter-vertebral discs of 12-week-old WT mice by immuno-fluoresce staining. OPG positive cells were observed in the endplate cartilage and annulus fibrosis, but not in the nucleus pulposus cells (Fig. 1). To determine if OPG plays a critical role in maintaining the integrity of IVD during aging, we assessed the morphology of the IVD tissues in 12, 20 and 28-week-old *OPG*$^{-/-}$ mice and their WT littermates. Although there was no global difference between WT and *OPG*$^{-/-}$ mice (Fig. 2A), we observed appearance of bone-like tissues in 20 and 28-week-old *OPG*$^{-/-}$ mice (Fig. 2B). The composition of bone-like-tissues is similar to those in ectopic bone formation, containing bone marrow, hematopoietic lineage cells, osteoclasts and mineralized bones. These bony tissues were inserted between the annulus fibrosis and the endplate cartilage, which are localized at the out layer of the IVD units. These abnormal bony tissues become more obvious in 28 week-old *OPG*$^{-/-}$ mice. Histomorphometric analyses revealed a reduction of the height of growth plates in all age groups of *OPG*$^{-/-}$ mice (Fig. 2C). A significantly loss of cartilage was observed in 20 and 28-old *OPG*$^{-/-}$ mice (Fig. 2D).

Contrast to these small histomorphometric difference between *OPG*$^{-/-}$ and WT mice, the area of abnormal bony tissues was significantly increased in *OPG*$^{-/-}$ mice (Fig. 3A), especially in 28-week-old mice. To investigate if these morphologic changes affect IVD function, we examined the expression levels of *aggrecan*, a chondrocyte-produced proteoglycan that is essential for cartilage integrity, in RNA isolated from IVD and adjacent endplate cartilages. We detected a significantly decreased *aggrecan* in *OPG*$^{-/-}$ mice at all time points. In contrast, *mmp13 and Col10* expression was unchanged at 12-week-old, but it was markedly increased in samples from 20 and 28-week-old *OPG*$^{-/-}$ mice (Fig. 3B). To determine if there is cellular damage, we performed TUNEL staining to identify apoptotic cells and demonstrated an increased apoptotic cells in IVD sections of 28-week-old *OPG*$^{-/-}$ mice (Fig. 3C). These data suggest that in the absence of OPG, IVD and endplate cartage tissues become abnormal and perhaps undergo early degenerative changes.

Active bone remodeling at the endplate cartilage of *OPG*$^{-/-}$ mice

Closer observation of IVD sections revealed that in some severe cases, partial endplate cartilage was lost and replaced by bony tissues (comparison between boxed area in WT and *OPG*$^{-/-}$ mice, Fig. 4A). Numerous of osteoblasts can be seen within bone marrow cavity on the inner surface of newly formed bony tissues (Fig. 4A, arrows). RT-PCR of total RNA extracted from IVD and adjacent endplate cartilage showed that the expression levels of *ALP*, *osteoterix*, and *osteocalcin* was significantly decreased in *OPG*$^{-/-}$ mice compared to those of WT at 12 weeks of age. The levels were elevated when mice became older. 28-week-old *OPG*$^{-/-}$ mice have 7-fold increased osteoclacin expression than WT tissues (Fig. 4B). Type I collagen immunostaining revealed no positive staining in cartilage endplate of WT mice at any time point. However, a clear positive staining was observed in bony tissues in the endplate cartilage of 20 and 28-old *OPG*$^{-/-}$ mice (Fig. 4C, arrows). Similarly, TRAP staining did not detect any TRAP+ osteoclasts in the endplate cartilage of WT mice, but numerous TRAP+ osteoclasts were seen at the bone edge. Interestingly, we also observed some osteoclasts that were invading into adjacent cartilage matrix (Fig. 5A, arrows). Corresponding to increased osteoclasts, we detected increased expression levels of osteoclast marker genes, *trap* and *rank*, in *OPG*$^{-/-}$ IVDs. The expression levels of catalytic enzymes *mmp9* and *cathepsin K* were also increased in *OPG*$^{-/-}$ mice (Fig. 5B).

Discussion

In this study, we examined the phenotype changes of intervertebral disc (IVD) including the endplate cartilage in 12 to 28 week-old $OPG^{-/-}$ mice and demonstrated that in the absence of OPG expression, a portion of the endplate cartilage is lost and replaced by newly formed bone marrow cavity. This change disrupts normal IVD structure, evidenced by decreased *aggrecan* and increased *mmp13* and *Col10* expression. The newly formed bone marrow cavity consists of osteoblasts and osteoclasts. The expression levels of markers and functional genes for these cell types are increased in the IVD tissues of $OPG^{-/-}$ mice. Furthermore, osteoclasts can be seen near or are invading the endplate cartilage in $OPG^{-/-}$ IVDs. These findings suggest that OPG plays an important role in maintaining the integrity of IVDs during the aging process.

OPG is a strong inhibitor of osteoclast formation by binding to RANKL and preventing RANKL from interaction of RANK. $OPG^{-/-}$ mice exhibit osteoporosis and osteoarthritis in knee joints with increased osteoclastogenesis [10–12]. However, if OPG plays a role in maintaining integrity of IVD during aging thereby contributing to disc disease has not been investigated. We found that in WT mice, OPG expresses at endplate cartilage and annulus fibrosis, but not in nucleus pulposus, which is consistent with the previous report in human intervertebral disc [8]. Cells in the endplate cartilage and annulus fibrosis are derived from mesenchymal cells while the nucleus pulposus cells are derived from notochordal cells [13]. Different original of these tissues may explain the differential expression pattern of OPG.

The deficiency of OPG gene leads to enhanced osteoclastogenesis, and secondary hyperactive osteoblasts in long bones [10–12]. We found this may be also the case in the vertebral bones. We observed numerous TRAP+ osteoclasts at the endplate cartilages of 20-week-old or even older $OPG^{-/-}$ mice, where no osteoclasts are normally present. Thus it is very likely that the normal function of OPG in IVD tissues is to inhibit the development of osteoclast lineage cells at these areas. A recent study reported that the deletion of OPG gene results in increased number of chondroclasts that present at the chondroosseous junctions at the fracture sites. These chondroclasts resorb the cartilaginous callus, thereby increasing the rate of fracture healing by accelerating local bone remodeling [14]. However, the precise cell types that are responsible for removing calcified cartilage during cartilage remodeling have not been well characterized. In 1962, Takuma S., for the first time, described a cell type that destroy and resorb cartilage, named them as chondroclasts. This type of cells also be later named as mineraloclasts and collagenoclasts [15,16]. Based on morphological and histo-chemical findings, these cells are usually taken to be the same as osteoclasts, which resorb bone and calcified cartilage. Using electronic microscopy, Nordahl et al found that chondroclasts do not form ruffled borders and clear zone, but they are TRAP positive [17]. However, until now, there is no function assay or specific marker available to distinguish chondroclasts from osteoclasts. Interestingly, mice with osteoclast deficient, such as c-fos [18], RANK [19], RANKL [20] and NF-κB p50/p52 double knockout mice [21], are often dwarfed and have abnormal growth plate phenotype, linking osteoclasts or/and chondroclasts to cartilage remodeling.

$OPG^{-/-}$ mice provide a valuable mode to investigate the role of osteoclasts/chondroclasts on cartilage remodeling. Increased cartilage loss in OPG−/− mice further confirms the importance of osteoclast in cartilage biology. It appears that the major consequence of osteoclast inhibition on cartilage is to cause dwarfism due to inhibited cartilage remodeling at the chondroosseous junctions [18–21]. This mechanism is more relevant in children. Abnormal knee joint [11] and IVD function (this study) in $OPG^{-/-}$ mice highlight the important role of osteoclast activation in cartilage remodeling.

An intact endplate cartilage is essential for normal IVD functions because the major nutrient supply of IVDs is diffused through endplates [22–23]. Pathologic changes in endplate cartilage are closely associated with IVD degeneration, leading to disc herniation, scoliosis, and spondylosis [24–25]. Loss of endplate cartilage and formation of new bone marrow cavity in $OPG^{-/-}$ mice points the importance of OPG expression in the maintaining normal IVD. This hypothesis is supported by significantly reduced expression of aggrecan, extra matrix protein critical for the normal disc [26–31]. in $OPG^{-/-}$ IVDs. Furthermore, because we found that apoptosis of chondrocytes only occurs in 28-week-old mice while cartilage loss and changes in the gene expression happens at 20-week-old mice, suggesting that that the deletion of OPG gene will not affect the apoptosis and hypertrophy of chondrocyte at early age, but with aging, the invading of osteoclast in the endplate could cause chondrocyte apoptosis and thus accelerate IVD degeneration.

Conclusion

The deletion of OPG gene causes the endplate cartilage resorption by hyperactive osteoclasts/chondroclasts. Alternation of OPG levels in the IVD may be a new mechanism of developing degenerative disc diseases by increasing osteoclasts-mediated cartilage resorption at the endplates.

Acknowledgments

This work was supported by the National Science Fund for Distinguished Young Scholars (30625043), the International Cooperation Programs of National Natural Science Foundation of China (30710103904), National Basic Research Program of China (973 Program 2010CB530400), the international technical cooperation key project plan, Chinese Science and Technology Committee Emphasis (2006DFA32670), the Project of National Natural Science Foundation of China (30930111, 30973760, 30901914, 30600829, 30701118 & 30572398), Changjiang Scholar Chair Professor project (Teach people [2009] 17), Shanghai Medical leading talent support scheme (LJ06018), Shanghai Education Innovation Project (08YZ56), The basic key project of Shanghai Science and Technology Commission (07JC14050), Shanghai Youth Science and Technology Development plan project (07QA14051, 09QA1405600), Shanghai University Innovation Team Programme (Shanghai Education Commission, Division 6 [2009]), The Ministry of Education Doctoral Fund (20070268004), Modernization of Chinese medicine - Shanghai Science and Technology Commission special (09dZ1977200), Shanghai university select and train outstanding young teachers in special fund (szy09021), Natural Science Foundation of Shanghai (11ZR1437100), National Institutes of Health PHS awards (AR48697 to LX).

Abbreviations

IVD	intervertebral disc
OPG	osteoprotegerin
TRAP	Tartrate-resistant acid phosphatase
TUNEL	Terminal deoxynucleotidyl transferase dUTP nick end labeling
ALP	Alkaline phosphatase
MMP9	Matrix metallopeptidase 9
MMP13	Matrix metallopeptidase 13
RANK	Receptor activator of nuclear factor kappa-B
RANKL	Receptor activator of nuclear factor kappa-B ligand
WT	wild type mice
HE	Haematoxylin and Eosin

References

1. Weiler C, Nerlich AG, Schaaf R, Bachmeier BE, Wuertz K, Boos N. Immunohistochemical identification of notochordal markers in cells in the aging human lumbar intervertebral disc. Eur Spine J. Epub ahead of print.
2. Cummings SR, Kelsey JL, Nevitt MC, O'Dowd KJ. Epidemiology of osteoporosis and osteoporotic fractures. Epidemiol Rev. 1985; 7:178–208. [PubMed: 3902494]
3. Pollintine P, Dolan P, Tobias JH, Adams MA. Intervertebral Disc Degeneration Can Lead to "Stress-Shielding" of the Anterior Vertebral Body: A Cause of Osteoporotic Vertebral Fracture? Spine (Phila Pa 1976). 2004; 29(7):774–782. [PubMed: 15087801]
4. Gruber HE, Gordon B, Williams C, Norton HJ, Hanley EN Jr. Correlation Between Bone Mineral Density and Intervertebral Disc Degeneration. Spine (Phila Pa 1976). 2007; 32(23):2529–236. [PubMed: 17978650]
5. Boyle WJ, Simonet WS, Lacey DL. Osteoclast differentiation and activation. Nature. 2003; 423(6937):337–342. [PubMed: 12748652]
6. Mitchner NA, Harris ST. Current and emerging therapies for osteoporosis. J Fam Pract. 2009; 58(7 Suppl)Osteoporosis. :S45–49.
7. Kwan Tat S, Amiable N, Pelletier JP, Boileau C, Lajeunesse D, Duval N, et al. Modulation of OPG, RANK and RANKL by human chondrocytes and their implication during osteoarthritis. Rheumatology (Oxford). 2009; 48(12):1482–1490. [PubMed: 19762475]
8. Mackiewicz Z, Salo J, Konttinen YT, Kaigle Holm A, Indahl A, Pajarinen J, et al. Receptor activator of nuclear factor kappa B ligand in an experimental intervertebral disc degeneration. Clin Exp Rheumatol. 2009; 27(2):299–306. [PubMed: 19473572]
9. Spahni AI, Schawalder P, Rothen B, Bosshardt DD, Lang N, Stoffel MH. Immunohistochemical localization of RANK, RANKL and OPG in healthy and arthritic canine elbow joints. Vet Surg. 2009; 38(6):780–786. [PubMed: 19674422]
10. Bucay N, Sarosi I, Dunstan CR, Morony S, Tarpley J, Capparelli C, et al. osteoprotegerin-deficient mice develop early onset osteoporosis and arterial calcification. Genes Dev. 1998; 12:1260–1268. [PubMed: 9573043]
11. Mizuno A, Amizuka N, Irie K, Murakami A, Fujise N, Kanno T, et al. Severe osteoporosis in mice lacking osteoclastogenesis inhibitory factor/osteoprotegerin. Biochem Biophys Res Commun. 1998; 247:610–615. [PubMed: 9647741]
12. Nakamura M, Udagawa N, Matsuura S, Mogi M, Nakamura H, Horiuchi H, et al. Osteoprotegerin regulates bone formation through a coupling mechanism with bone resorption. Endocrinology. 2003; 144:5441–5449. [PubMed: 14500574]
13. Hunter CJ, Matyas JR, Duncan NA. The Notochordal Cell in the Nucleus Pulposus: A Review in the Context of Tissue Engineering. Tissue Eng. 2003; 9(4):667–677. [PubMed: 13678445]
14. Ota N, Takaishi H, Kosaki N, Takito J, Yoda M, Tohmonda T, et al. Accelerated cartilage resorption by chondroclasts during bone fracture healing in osteoprotegerin-deficient mice. Endocrinology. 2009; 150(11):4823–4834. [PubMed: 19819969]
15. TAKUMA S. Electron Microscopy of Cartilage Resorption by Chondroclasts. J Dent Res. 1962; 41:883–889. [PubMed: 13919289]
16. Knese KH. Osteoclasts, chondroclasts, mineraloclasts, collagenoclasts. Acta Anat (Basel). 1972; 83(2):275–288. [PubMed: 5085474]
17. Nordahl J, Andersson G, Reinholt FP. Chondroclasts and osteoclasts in bones of young rats: comparison of ultrastructural and functional features. Calcif Tissue Int. 1998; 63(5):401–408. [PubMed: 9799825]
18. Wang, Zhao-Qi; Ovitt, Catherine; Grigoriadis, Agamemnon E.; Möhle-Steinlein, Uta; Rüther, Ulrich; Wagner, Erwin F. Bone and haematopoietic defects in mice lacking c-fos. Nature. 1992; 360(6406):741–745. [PubMed: 1465144]
19. Li J, Sarosi I, Yan XQ, Morony S, Capparelli C, Tan HL, McCabe S, Elliott R, Scully S, Van G, Kaufman S, Juan SC, Sun Y, Tarpley J, Martin L, Christensen K, McCabe J, Kostenuik P, Hsu H, Fletcher F, Dunstan CR, Lacey DL, Boyle WJ. RANK is the intrinsic hematopoietic cell surface

receptor that controls osteoclastogenesis and regulation of bone mass and calcium metabolism. Proc Natl Acad Sci U S A. 2000; 97(4):1566–1571. [PubMed: 10677500]

20. Odgren PR, Kim N, MacKay CA, Mason-Savas A, Choi Y, Marks SC Jr. The role of RANKL (TRANCE/TNFSF11), a tumor necrosis factor family member, in skeletal development: effects of gene knockout and transgenic rescue. Connect Tissue Res. 2003; 44 (Suppl 1):264–271. [PubMed: 12952207]
21. Xing, L.; Yamashita, T.; Childs, L.; Schwarz, EM.; O'Keefe, RJ.; Dougall, WC.; Boyce, BF. RANKL/RANK/NF-kB Signaling Regulates Chondrogenesis. Concurrent Oral Session C20 of The 24th Annual meeting of the American Society for Bone and Mineral Research; San Antonio, TX, USA. September, 2002;
22. Katz MM, Hargens AR, Garfin SR. Intervertebral disc nutrition: diffusion versus convection. Clin Orthop Relat Res. 1986; 210:243–245. [PubMed: 3757370]
23. Urban JP, Smith S, Fairbank JC. Nutrition of the intervertebral disc. Spine. 2004; 29:2700–2709. [PubMed: 15564919]
24. Holm S, Holm AK, Ekström L, Karladani A, Hansson T. Experimental disc degeneration due to endplate injury. J Spinal Disord Tech. 2004; 17(1):64–71. [PubMed: 14734978]
25. Turgut M, Uslu S, Uysal A, Yurtseven ME, Ustün H. Changes in vascularity of cartilage endplate of degenerated intervertebral discs in response to melatonin administration in rats. Neurosurg Rev. 2003; 26(2):133–138. [PubMed: 12962300]
26. Oegema TR Jr. The role of disc cell heterogeneity in determining disc biochemistry: a speculation. Biochem Soc Trans. 2002; 30:839–844. [PubMed: 12440929]
27. Sive JI, Baird P, Jeziorsk M, Watkins A, Hoyland JA, Freemont AJ. Expression of chondrocyte markers by cells of normal and degenerate intervertebral discs. Mol Pathol. 2002; 55:91–97. [PubMed: 11950957]
28. Yang CL, Rui H, Mosler S, Notbohm H, Sawaryn A, Müller PK. Collagen II from articular cartilage and annulus fibrosus: structural and functional implication of tissue specific posttranslational modifications of collagen molecules. Eur J Biochem. 1993; 213:1297–302. [PubMed: 8504821]
29. Roughley PJ. Biology of intervertebral disc aging and degeneration: involvement of the extracellular matrix. Spine. 2004; 29:2691–2699. [PubMed: 15564918]
30. Roughley PJ, Alini M, Antoniou J. The role of proteoglycans in aging, degeneration and repair of the intervertebral disc. Biochem Soc Trans. 2002; 30:869–874. [PubMed: 12440935]
31. Cs-Szabo G, Ragasa-San Juan D, Turumella V, Masuda K, Thonar EJ, An HS. Changes in mRNA and Protein Levels of Proteoglycans of the Anulus Fibrosus and Nucleus Pulposus During Intervertebral Disc Degeneration. Spine. 2002; 27:2212–2219. [PubMed: 12394896]

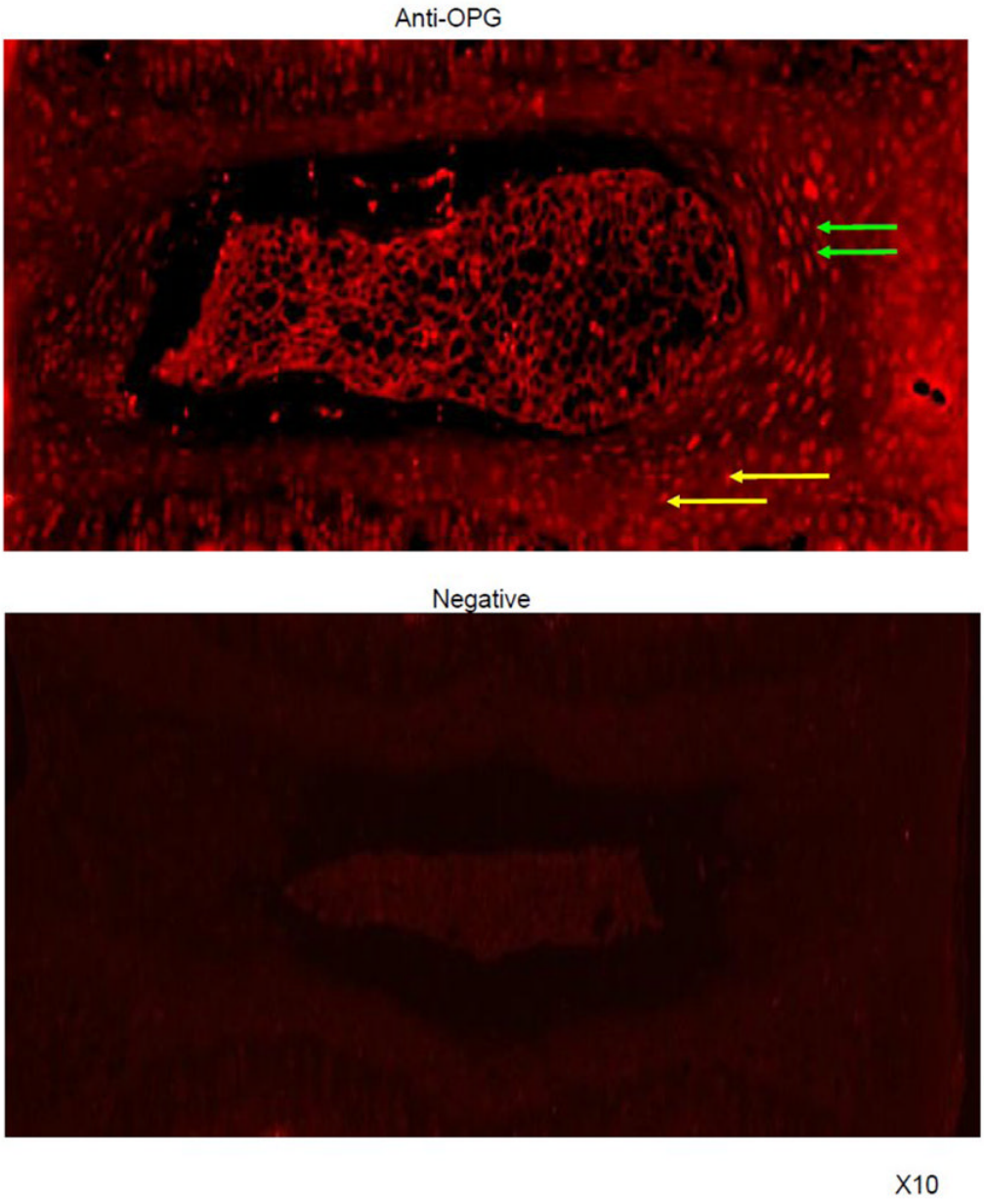

Figure 1. Immuno-fluorescence staining of OPG in vertebral bones of a WT mouse

C4–6 vertebral bodies from 12-week-old WT mice were stained with anti-OPG antibody. Positive OPG staining was observed in the annulus fibrosis (green arrows) and the endplate cartilage (yellow arrows). Photos (x10) are the representative staining from 3 mice.

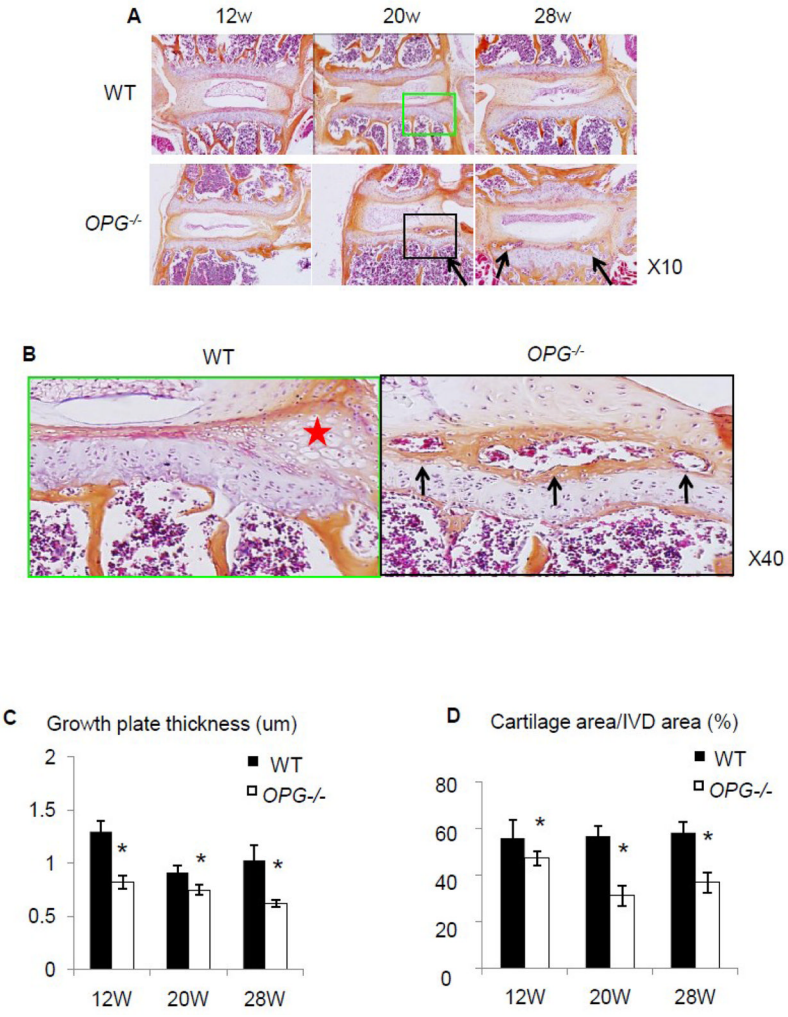

Figure 2. Abnormal vertebral bones of *OPG*$^{-/-}$ mice

(A) Hematoxylin eosin staining of IVD and endplate cartilage of 12-, 20- and 28-week-old WT and *OPG*$^{-/-}$ mice. Arrows indicate the bone-like tissue formation. (B) Enlargement of tissues highlighted in boxed area in A, demonstrating bone marrow formation (arrows). The cartilage area was indicated by red star. (C) Histomoprhometric assessment of growth plate thickness and cartilage area. Values are the mean ± SD of 3 mice. Three sections per mouse were analyzed. *p< 0.05 vs. WT group.

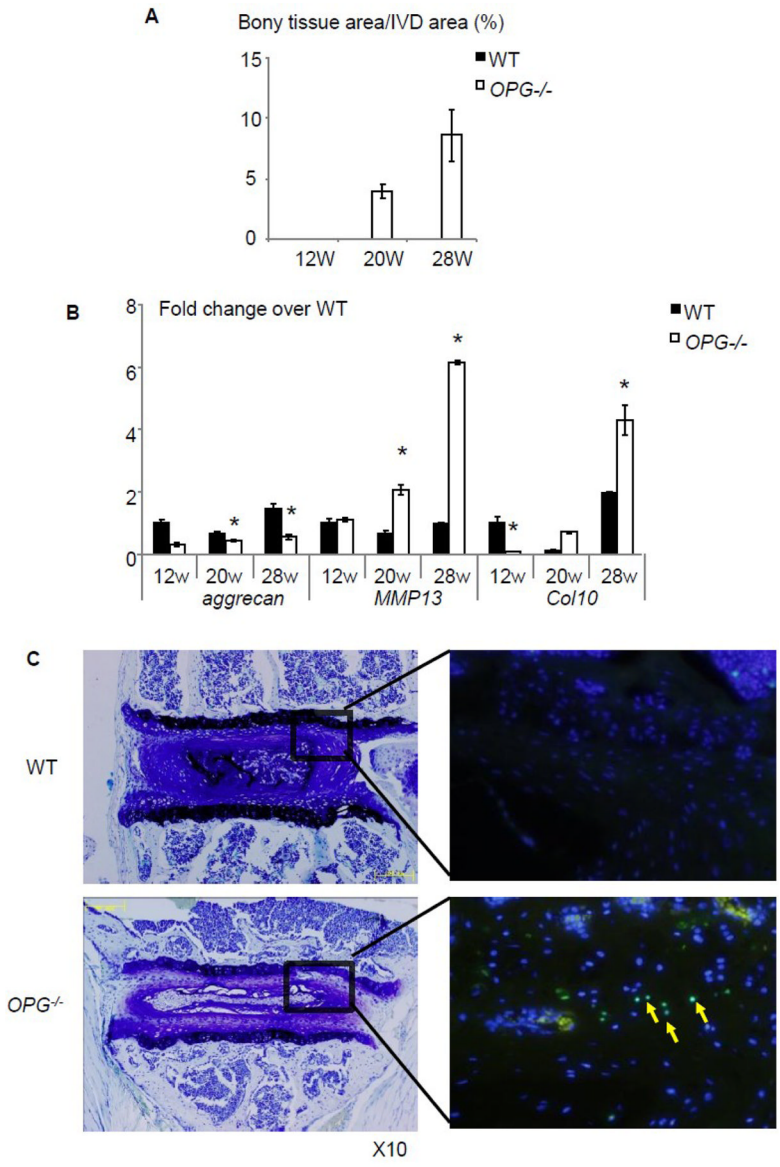

Figure 3. Impaired IVD in *OPG*$^{-/-}$ mice

(A) Histomoprhometric assessment of newly formed bony tissues in endplate of 12-, 20- and 28-week-old WT and *OPG*$^{-/-}$ mice. Values are the mean ± SD of 3 mice. Three sections per mouse were analyzed. (B) The expression levels of *aggrecan*, *mmp13* and *Col10* mRNA in RNA extracted from IVD and endplate cartilages of 12-, 20- and 28-week-old WT and *OPG*$^{-/-}$ mice. The values are the mean ± SD of 3 independent experiments. *p< 0.05 vs. WT group. (C) TUNEL staining of IVDs of 28-week-old *OPG*$^{-/-}$ mice and WT littermates. Left photos are toludine blue stained sections and the right photos are the TUNEL stained adjacent sections. Apoptotic cells were indicated by yellow arrows.

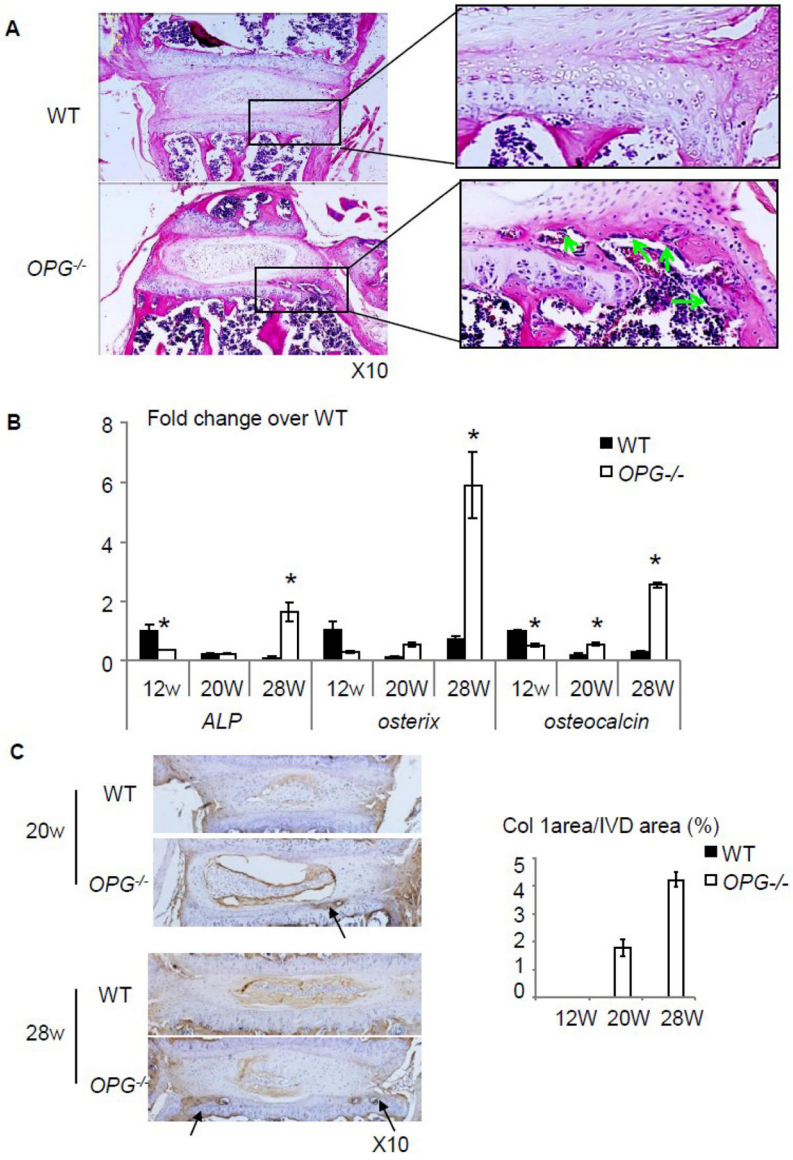

Figure 4. Bone formation in the endplate of *OPG*$^{-/-}$ mice

(A) H&E sections show newly formed bone marrow cavity in the endplate cartilage in *OPG*$^{-/-}$ mice. Osteoblasts were indicated by green arrows. (B) mRNA expression of *ALP*, *osteocalcin*, and *osterix* of intervertebral discs of WT and *OPG*$^{-/-}$ mice at all time points. The values are the mean ± SD of 3 independent experiments. **p* <0.05 vs WT group. (C) Type I collagen immunostaining of IVD sections of 20 and 28-week-old WT and *OPG*$^{-/-}$ mice. Arrow indicates positive type I collagen staining in the endplate cartilage. Bar graphs are the % of positive stained area over IVD area. Values are the mean ± SD of 3 mice. One section per mouse were analyzed.

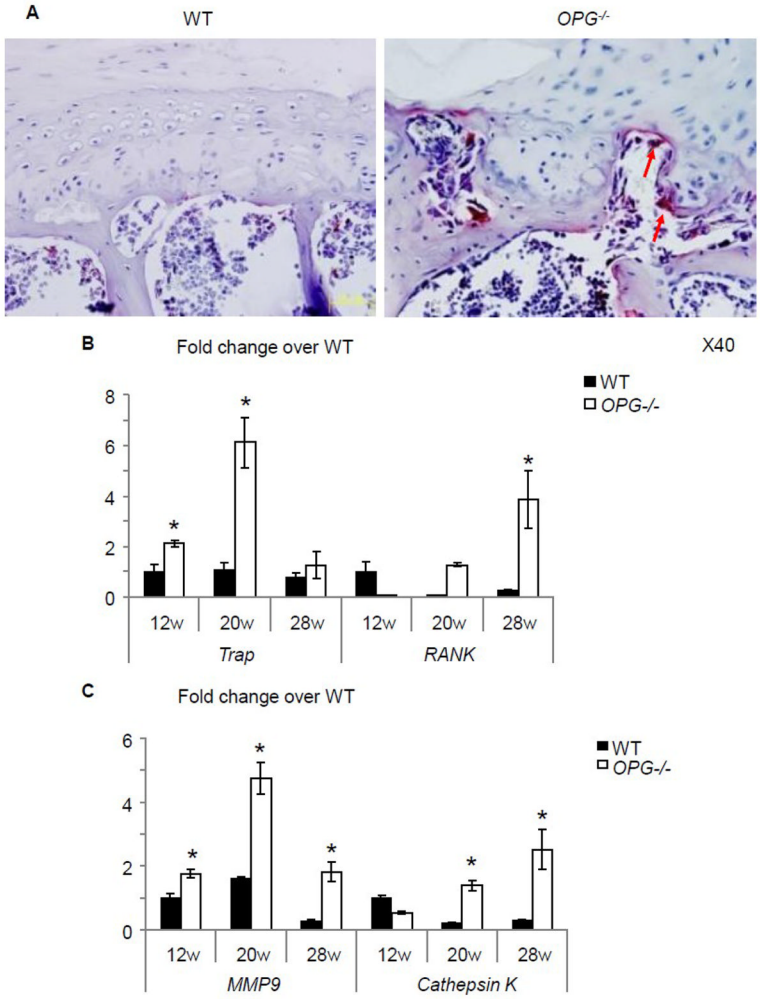

Figure 5. Osteoclasts in the endplate of *OPG*$^{-/-}$ mice

(A) TRAP staining of vertebral body 28-week-old of *OPG*$^{-/-}$ mice and WT littermates (x40). Arrows indicate osteoclasts invading into cartilage matrix. (B) mRNA expression of *trap*, *rank*, *mmp9* and *cathepsin K* in RNA extracted from IVD and endplate cartilages of WT and *OPG*$^{-/-}$ mice at 12, 20 and 28-week-old. Values are the mean ± SD of 3 independent experiments. **p* <0.05 vs WT group.

Table 1

Sequences of primers used in the Real-time RT-PCR

Name	GenBank accession no.		Sequnce(5′-3′)
β-actin	NM_007393.3	Forward	GGAGATTACTGCCCTGGCTCCTA
		Reverse	GACTCATCGTACTCCTGCTTGCTG
aggrecan	NM_007424.2	Forward	CGCCACTTTCATGACCGAGA
		Reverse	TCATTCAGACCGATCCACTGGTAG
osteocalcin	NM_001032298.2	Forward	CTTGAAGACCGCCTACAAAC
		Reverse	GCTGCTGTGACATCCATAC
osterix	NM_130458.3	Forward	CGCATCTGAAAG CCCACTTG
		Reverse	CAGCTCGTCAG AGCGAGTGAA
TRAP	NM_007388.3	Forward	TTGCGACCATTGTTAGCCACATA
		Reverse	TCAGATCCATAGTGAAA CCGCAAG
MMP9	NM_013599.2	Forward	CCATGCACTGGGCTTAGATCA
		Reverse	GGCCTTGGGTCAGGCTTAGA
RANK	NM_009399.3	Forward	ATGGTGGGCTACCCAGGTGA
		Reverse	ACTTGCGGCTGCACAGTGA
cathepsin K	NM_007802.3	Forward	CAGCAGAACGGAGGCATTGA
		Reverse	CTTTGCCGTGGCGTTATACATACA
MMP13	NM_008607.2	Forward	ACTTTGTTGCCAATTCCAGG
		Reverse	TTTGAGAACACGGGGAAGAC
Col 10	NM_009925.4	Forward	ACCCCAAGGACCTAAAGGAA
		Reverse	CCCCAGGATACCCTGTTTTT
ALP	NM_007431.2	Forward	ACACCTTGACTGTGGTTACTGCTGA
		Reverse	CCTTGTAGCCAGGCCCGTTA

Note: *TRAP*: Tartrate-resistant acid phosphatase; *ALP*: Alkaline phosphatase; *MMP9*: Matrix metallopeptidase 9; *MMP13*: Matrix metallopeptidase 13; *RANK*: Receptor activator of nuclear factor kappa-B; *Col 10:* Type X collagen.